Molecular and Cellular Biomedical Sciences, Vol.10 No.1, March 2026, p. 1-70
Print ISSN: 2527-4384, Online ISSN: 2527-3442
DOI: 10.21705/mcbs.v10n1.749

RESEARCH ARTICLE

MCBS
Mol Cell Biomed Sci. 2026; 10(1): 55-64
DOI: 10.21705/mcbs.v10n1.749

# Hypoxia-Conditioned MSC Exosomes Upregulate mTORC1 and Suppress MMP-2 in a UV-B–Induced Collagen Loss Rat Model

Anggrila Sekar Fadhillah[1], Agung Putra[2,3,4], Titiek Sumarawati[4], Eko Setiawan[1,5]

[1]*Department of Postgraduate Biomedical Science, Faculty of Medicine, Universitas Islam Sultan Agung, Semarang, Indonesia*
[2]*Stem Cell and Cancer Research (SCCR) Laboratory, Faculty of Medicine, Universitas Islam Sultan Agung, Semarang, Indonesia*
[3]*Department of Pathological Anatomy, Faculty of Medicine, Universitas Islam Sultan Agung, Semarang, Indonesia*
[4]*Department of Doctoral Biomedical Science, Faculty of Medicine, Universitas Islam Sultan Agung, Semarang, Indonesia*
[5]*Department of Surgery, Faculty of Medicine, Universitas Islam Sultan Agung, Semarang, Indonesia*

**Background:** Ultraviolet-B (UV-B) radiation accelerates photoaging by disrupting extracellular matrix (ECM) homeostasis through dysregulation of mechanistic target of rapamycin complex 1 (mTORC1) and upregulation of matrix metalloproteinase-2 (MMP-2). This study evaluated the effects of exosomes of hypoxia-conditioned mesenchymal stem cells (EH-MSCs) on mTORC1 and MMP-2 expression in a UV-B–induced collagen loss rat model.

**Materials and methods:** Thirty male Wistar rats were randomized into five groups: healthy control, UV-B + saline, UV-B + hyaluronic acid, UV-B + 200 µL EH-MSCs, and UV-B + 300 µL EH-MSCs. Collagen loss was induced by UV-B irradiation for two weeks (10 sessions, 8 min/session). A single treatment was administered on day 22, and tissue was collected on day 29. Exosomes were isolated from hypoxia-conditioned MSCs and characterized by morphology and surface markers. Gene expression of mTORC1 and MMP-2 was assessed by qRT-PCR and analyzed using one-way ANOVA.

**Results:** UV-B exposure induced collagen loss histologically. EH-MSCs significantly increased mTORC1 expression, highest in the 300 µL group ($p < 0.001$), and reduced MMP-2 expression, lowest in the 300 µL group.

**Conclusion:** EH-MSCs exert dual regulatory effects by upregulating mTORC1 and suppressing MMP-2 in UV-B–induced collagen loss, suggesting therapeutic potential to mitigate photoaging via anabolic signaling (via mTORC1) and reduced ECM degradation (via MMP-2).

**Keywords:** *collagen loss, exosomes, MMP-2, mTORC1, UV-B*

## Introduction

Ultraviolet-B (UV-B) radiation is a major extrinsic factor that contributes to premature skin aging, also known as photoaging. Clinical manifestations of photoaging include dryness, wrinkles, roughness, and pigmentation disorders, which account for nearly 80% of visible aging signs in skin.[1] Global studies report dry skin prevalence ranging from 29%

Submission: October 2, 2025
Last Revision: January 8, 2026
Accepted for Publication: January 29, 2026

**Corresponding Author**:
Eko Setiawan
Department of Surgery, Faculty of Medicine
Universitas Islam Sultan Agung
Terboyo Kulon, Semarang 50112, Indonesia
e-mail: drekosetiawan@unissula.ac.id

to 85%, with data from Indonesia reaching 50%–80%.[2,3] Chronic UV-B exposure disrupts redox balance through excessive reactive oxygen species (ROS) generation, which damages DNA, lipids, and proteins, leading to persistent inflammation.[4,5] This process accelerates degradation of the extracellular matrix (ECM) by increasing the activity of matrix metalloproteinases (MMPs), enzymes responsible for collagen and elastin breakdown.[6,7] In particular, MMP-2, a gelatinase responsible for degrading collagen and other matrix proteins, is upregulated by UV-B radiation.[8,9] Exposure to UV-B radiation also disrupts key molecular pathways, including the mechanistic target of rapamycin complex 1 (mTORC1), which plays a central role in maintaining skin homeostasis. Dysregulation of mTORC1 accelerates ECM degradation, with a rate of degradation two to four times faster than under normal conditions, leading to increased collagen loss and accelerated skin aging.[10] mTORC1 acts as a central regulator of cellular metabolism, protein synthesis, and autophagy, and its imbalance is associated with pathological processes of senescence and degeneration.[11,12] Physiological activation of mTORC1 supports protein synthesis and collagen production in dermal fibroblasts, thereby contributing to ECM renewal and repair, whereas UV-B–induced dysregulation shifts this pathway toward maladaptive signaling.[10–12] Together, hyperactivation of MMPs and aberrant mTORC1 represent critical mechanisms underlying UV-B–mediated skin photoaging.

Therapeutic interventions targeting oxidative stress and ECM degradation are actively explored to counter photoaging. Exosomes are nanoscale extracellular vesicles released by most cell types, characterized by a lipid bilayer membrane and a cargo of proteins, lipids, and nucleic acids that mediate intercellular communication and can be exploited as diagnostic and therapeutic tools.[13,14] In particular, mesenchymal stem cell–derived exosomes (E-MSCs) have demonstrated regenerative potential by protecting against oxidative stress–induced tissue injury and activating endogenous repair pathways, supporting their development as promising candidates for regenerative medicine applications.[15,16] In dermatology, exosomes protect against UV-B–induced oxidative stress, restore collagen synthesis, and suppress MMP expression, thereby improving skin elasticity and structure.[17,18] Importantly, hypoxia-conditioned MSCs produce exosomes with enhanced paracrine activity, boosting angiogenesis, antioxidant defense, and tissue repair compared to normoxic conditions.[19,20]

Despite these advances, few studies have investigated the dual regulatory effect of exosomes of hypoxia-conditioned MSC (EH-MSCs) on both mTORC1 and MMP-2 in UV-B–induced collagen loss. Previous research has largely focused on exosome effects on general photoaging markers, collagen gene expression, or histopathological parameters.[17,18] Other studies describe the role of mTORC1 in regulating exosome release or the contribution of exosome-derived circ_MMP2 in cancer metastasis but the combined evaluation of mTORC1 and MMP-2 modulation in a UV-B model remains limited.[21,22] This knowledge gap restricts understanding of whether EH-MSCs act through simultaneous activation of mTORC1 and inhibition of MMP-2 to restore ECM homeostasis under oxidative stress conditions.

Therefore, this study aims to evaluate the effect of EH-MSC administration on mTORC1 and MMP-2 gene expression in male Wistar rats exposed to UV-B radiation. By directly comparing treated and untreated groups in a collagen loss model, the study investigates the potential of EH-MSCs as a dual-action therapy that upregulates mTORC1 while downregulating MMP-2. The novelty of this work lies in establishing a molecular mechanism that links EH-MSCs to both anabolic and anti-catabolic pathways of ECM regulation, providing evidence for exosome-based strategies to prevent or attenuate photoaging.

## Materials and methods

### *Study Design*

The research applied a true experimental method with a randomized post-test–only design incorporating control groups. The objective was to examine the effect of EH-MSCs on mTORC1 and MMP-2 expression in a rat model of collagen loss induced by UV-B radiation. The research was conducted at the Stem Cell and Cancer Research (SCCR) Laboratory, Faculty of Medicine, Universitas Islam Sultan Agung, Semarang, Indonesia. All procedures performed in this study were conducted in accordance with the ethical approval as stated in the ethical statement subsection.

### *Animal Models*

Thirty healthy male Wistar rats (Rattus norvegicus), aged 8–12 weeks and weighing between 200–250 g, were included in the study. Prior to treatment, the animals were allowed a one-week acclimatization period under standard laboratory conditions (temperature 22±2°C, humidity 55±10%, and a

Print ISSN: 2527-4384, Online ISSN: 2527-3442
DOI: 10.21705/mcbs.v10n1.749

12-h light/dark cycle) with unrestricted access to food and water.

***Sample Size and Grouping***

Rats were randomly divided into five groups (n = 6) (Figure 1). Group 1 (G1) was a healthy control without UV-B exposure. Groups 2–5 were exposed to UV-B radiation, followed by different interventions: Group 2 (G2) received 200 µL normal saline (Otsuka Pharmaceutical, Tokyo, Japan), Group 3 (G3) received 200 µL hyaluronic acid (Hyruan Plus®, LG Chem, Seoul, South Korea), Group 4 (G4) received 200 µL EH-MSCs, and Group 5 (G5) received 300 µL EH-MSCs. A volume of 200 µL was selected for saline, hyaluronic acid, and the lower-dose EH-MSC group to standardize the injection volume across groups and to ensure adequate dispersion within the dorsal skin without causing injection-related damage. The 300 µL EH-MSC dose was included as a higher-dose arm to explore a potential dose–response effect while remaining within a technically feasible and well-tolerated injection volume. These volumes' settings were also used in the previous studies.[23,24]

***Preparation of Exosomes***

Umbilical cord tissue was processed under aseptic conditions in a class II biosafety cabinet (ESCO, Singapore). After carefully removing blood vessels, the cords were rinsed with phosphate-buffered saline (PBS; Gibco, Thermo Fisher Scientific, USA), cut into small pieces, and distributed evenly into T25 culture flasks (Corning, USA). Explants were overlaid with a complete growth medium composed of Dulbecco's Modified Eagle Medium (DMEM; Gibco, Thermo Fisher Scientific, USA), supplemented with 10% fetal bovine serum (FBS; Gibco, Thermo Fisher Scientific, USA), 1% penicillin–streptomycin (Sigma-Aldrich, Merck KGaA, Germany), and 0.5% fungizone (Amphotericin B; Thermo Fisher Scientific, USA). Cultures were maintained at 37°C in a humidified incubator with 5% $CO_2$ (Binder GmbH, Germany), and the medium was renewed every three days. Fibroblast-like MSCs became visible after approximately 10–14 days, were expanded until approximately 80% confluence, and subcultured up to passage 4. The mesenchymal identity of these cells was confirmed by their spindle-shaped morphology, positive expression of CD90 and CD29 with low expression of CD45 and CD31 on flow cytometry, and their ability to undergo osteogenic and adipogenic differentiation.

For hypoxic preconditioning, MSCs at near confluence were transferred into a hypoxia chamber (STEMCELL Technologies, Canada) and maintained at 5% $O_2$ for 24 hours. Following incubation, the MSC-conditioned medium was harvested and clarified by sequential centrifugation: first at 300×g for 10 minutes to remove residual cells and large aggregates, then at 10,000×g for 30 minutes at 4°C to eliminate cell debris and larger vesicles. The resulting supernatant was subsequently subjected to ultracentrifugation at 100,000× for 70 minutes at 4°C using an Optima™ XPN ultracentrifuge (Beckman Coulter, USA) to pellet the exosome-enriched fraction. The resulting pellets were rinsed once with PBS (Gibco, Thermo Fisher Scientific, USA), resuspended in sterile PBS, and stored at –80°C until further analysis. Protein levels of the isolated exosomes were quantified with a bicinchoninic acid (BCA) protein assay kit (Pierce™, Thermo Fisher Scientific, USA). In this study, vesicles were operationally defined as MSC-derived exosomes based on their origin from MSC-conditioned medium and recovery in the 100,000×g ultracentrifugation fraction, in accordance with the MISEV2018 guidelines.[14] However, we did not perform additional characterization using canonical exosome surface markers (e.g., CD9, CD63, CD81, TSG101, ALIX), which we acknowledge as a methodological limitation.

***UV-B Irradiation Protocol***

Groups 2–5 were subjected to UV-B irradiation to induce collagen loss using a UV-B lamp (Philips TL 20W/12 RS, Eindhoven, Netherlands) at a wavelength of 302 nm positioned 20 cm above the dorsal surface. Exposure was carried out over two weeks (day 8–21) with a total of 10 sessions, administered five times per week, each lasting 8 minutes. On day 22, treatment interventions were given once according to group allocation. After a 7-day post-treatment period, the animals were sacrificed on day 29 for tissue collection.

***Tissue Collection and Gene Expression Analysis***

On day 29, animals were euthanized through an intraperitoneal injection of a lethal anesthetic mixture containing ketamine (50 mg/kg; Ketalar®, Pfizer, USA), xylazine (10 mg/kg; Bayer, Germany), and acepromazine

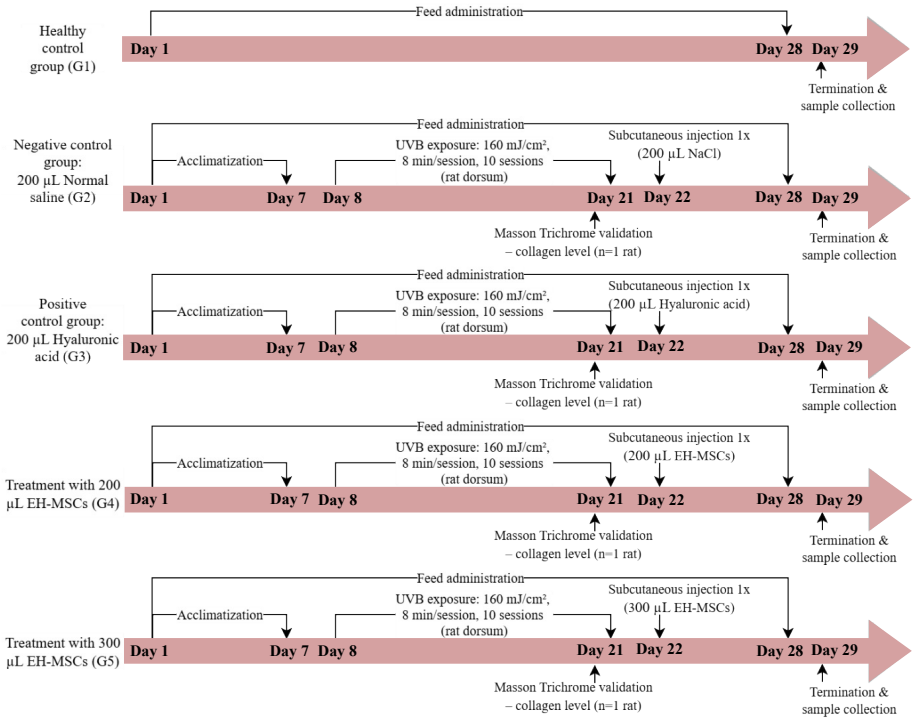


**Figure 1. Schematic diagram of the study design and experimental timeline.**

(2 mg/kg; Boehringer Ingelheim, Germany). To ensure death, cervical dislocation was performed immediately afterward. Dorsal skin from the UV-B–irradiated region was excised under sterile conditions. Part of each specimen was immersed in 10% neutral-buffered formalin (Sigma-Aldrich, Merck KGaA, Germany) for 24 hours, then transferred into 70% ethanol before paraffin embedding for histopathological examination using Masson's trichrome staining. The remaining tissue was placed in RNAlater™ solution (Invitrogen, Thermo Fisher Scientific, USA) and stored at –80 °C until molecular analysis.

RNA was extracted from preserved samples using TRIzol™ reagent (Invitrogen, Thermo Fisher Scientific, USA). Complementary DNA (cDNA) was synthesized with the RevertAid First Strand cDNA Synthesis Kit (Thermo Fisher Scientific, USA). Gene expression was quantified using real-time PCR with SYBR™ Green Master Mix (Applied Biosystems, Thermo Fisher Scientific, USA) on a QuantStudio™ 3 Real-Time PCR platform (Thermo Fisher Scientific, USA). The relative expression of mTORC1 and MMP-2 was assessed, with GAPDH serving as the reference gene (Table 1). Results were analyzed using the 2^-ΔΔCt

the RevertAid First Strand cDNA Synthesis Kit (Thermo Fisher Scientific, USA). Gene expression was quantified using real-time PCR with SYBR™ Green Master Mix (Applied Biosystems, Thermo Fisher Scientific, USA) on a QuantStudio™ 3 Real-Time PCR platform (Thermo Fisher Scientific, USA). The relative expression of mTORC1 and MMP-2 was assessed, with GAPDH serving as the reference gene (Table 1). Results were analyzed using the 2^-ΔΔCt method.

### *Statistical Analysis*

Data processing was carried out using SPSS software, version 26.0 (IBM Corp., Armonk, NY, USA). The Shapiro–Wilk test was employed to verify data normality, and variance homogeneity was examined with Levene's test. Differences among experimental groups were assessed by one-way analysis of variance (ANOVA). For post hoc comparisons, the Least Significant Difference (LSD) method was applied when homogeneity assumptions were satisfied, whereas Tamhane's T2 test was used when variances were unequal. A probability value of less than 0.05 was interpreted as statistically significant.

Print ISSN: 2527-4384, Online ISSN: 2527-3442
DOI: 10.21705/mcbs.v10n1.749

**Table 1. The primer sequences used for qRT-PCR amplification of mTORC1 and MMP-2 genes.**

| Expression | Properties |
|---|---|
| **mTORC1** | |
| Forward | 5'-TGA CTT ACC GAG AGC ACA CA-3' |
| Reverse | 5'-ACA TTC ACA GAC TCA GGC ATC-3' |
| Amplicon size | 120 bp |
| Temperature | 60°C |
| GC Content | 50% |
| **MMP-2** | |
| Forward | 5'-AAA GGA GGG CTG CAT TGT GAA-3' |
| Reverse | 5'-CTG GGG AAG GAC GTG AAG AGG-3' |
| Amplicon size | 150 bp |
| Temperature | 62°C |
| GC Content | 47.6% |
| **GADPH** | |
| Forward | 5'- GAA GGT GAA GGT CGG AGT-3' |
| Reverse | 5'- GAA GAT GGT GAT GGG ATT TC-3' |
| Amplicon size | 140 bp |
| Temperature | 57°C |
| GC Content | 50% |

## Results

### *Validation of Collagen Loss*

UV-B irradiation successfully induced collagen degradation in the rat model. Macroscopically, healthy rats showed smooth dorsal skin without erythema or wrinkling, whereas UV-B–exposed rats developed visible redness and prominent skin folds. Histological examination of dorsal skin using Masson's trichrome staining demonstrated a qualitative reduction in collagen in the UV-B–irradiated groups, evidenced by decreased blue staining intensity and collagen bundles that appeared thinner, more fragmented, and less compact within the superficial and mid-dermis compared with the densely packed, uniformly oriented fibers observed in healthy controls (Figure 1). Although collagen content was not quantified morphometrically in this study, the concordant macroscopic and microscopic changes consistently observed across animals support the successful induction of dermal collagen loss by the UV-B protocol (Figure 2).

### *Validation of EH-MSCs*

MSCs obtained from rat umbilical cord developed a spindle-shaped, fibroblast-like morphology after the fourth passage under hypoxic culture conditions (Figure 3). Their multipotency was verified through differentiation tests, where osteogenic induction produced calcium deposits that stained positively with Alizarin Red, and adipogenic induction generated lipid droplets visualized by Oil Red O (Figure 3). Flow cytometry analysis indicated strong expression of MSC surface markers CD90 (99.98%) and CD29 (99.96%), along with very low expression of hematopoietic markers CD45 (0.27%) and CD31 (0.40%). Although the International Society for Cell & Gene Therapy (ISCT) recommends CD73, CD90, and CD105 as core positive markers for human MSCs, in this study we evaluated CD90 and CD29 as positive markers and did not include CD73 or CD105 in our panel, which we acknowledge as a limitation of the phenotypic characterization. We also acknowledged the absence of chondrogenic differentiation assessment. Taken together with the demonstrated osteogenic and adipogenic differentiation capacity, these findings support the mesenchymal identity and purity of the hypoxia-conditioned MSC population (Figure 4).

### *EH-MSC Dose–Dependent Increase in mTORC1 and Decrease in MMP-2 Expression*

Expression of mTORC1 differed significantly among treatment groups. Rats exposed to UV-B and injected with saline (G2) showed the lowest mean expression (0.313±0.057), while the highest mean was observed in the group treated with 300 µL EH-MSCs (G5: 1.088±0.286). Intermediate values were recorded in the hyaluronic acid group (G3: 0.498±0.180) and the 200 µL EH-MSCs group (G4: 0.687±0.223). Group variability was found to be significant based on ANOVA results ($p$<0.001). Post hoc analysis showed that both exosome-treated groups (G4 and G5) had significantly higher mTORC1 expression compared with the saline group (G2), and G5 differed

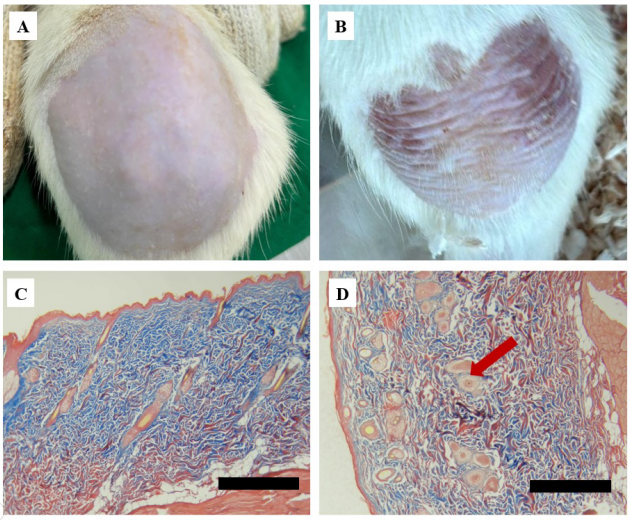


**Figure 2. Validation of collagen loss in UV-B–irradiated Wistar rats.** A: healthy skin without wrinkles, B: UV-B–exposed skin with visible wrinkling, C: abundant collagen in healthy rats, D: reduced collagen in UV-B–exposed rats stained with Masson's trichrome. The red arrow in (D) indicates a region in the dermis showing significant collagen loss and fragmentation following UV-B irradiation. Black bar: 10 µm.

significantly from all other groups (G2 vs G5, G3 vs G5, and G4 vs G5) (Table 2 and Figure 5).

MMP-2 expression showed an inverse pattern compared to mTORC1. The highest mean expression was recorded in the saline group (G2: 1.012±0.177), while the lowest was observed in the 300 µL EH-MSCs group (G5: 0.187±0.070). Intermediate values were found in the hyaluronic acid group (G3: 0.595±0.188) and the 200 µL EH-MSCs group (G4: 0.422±0.099). One-way ANOVA demonstrated that group comparisons were statistically significant ($p$<0.001). Post hoc tests indicated that both exosome-treated groups (G4 and G5) significantly reduced MMP-2 expression compared with the saline group (G2) (Table 2 and Figure 5).

## Discussion

This study demonstrated that administration of EH-MSCs significantly modulated mTORC1 and MMP-2 gene expression in male Wistar rats with UV-B–induced collagen loss (Table 2, Figure 5). The findings support the initial hypothesis that EH-MSCs exert protective effects against photoaging by simultaneously influencing anabolic and catabolic pathways of extracellular matrix regulation. The downregulation of MMP-2 observed in this study is consistent with the established role of UV-B radiation in enhancing matrix metalloproteinase activity, which accelerates collagen degradation and skin aging.[6,7] Exosome treatment, particularly at the 300 µL dose, produced a clear suppression of MMP-2 expression compared with saline and hyaluronic acid controls, confirming the anti-catabolic potential of EH-MSCs. This finding aligns with previous reports that MSC-derived exosomes reduce extracellular matrix breakdown by attenuating oxidative stress and downregulating MMP expression through activation of redox-sensitive pathways such as NRF2, ultimately preserving collagen structure in photoaged skin.[15,17] In parallel, a study reported that EH-MSCs modulated PKA and VEGFR in a UV-B–induced hyperpigmentation model, demonstrating their ability to regulate skin responses to UV-B damage.[25] Similarly, another study showed that E-MSCs enhanced FGF-1 and SDF-1 expression in burn injuries, further supporting their regenerative role in tissue damage models.[23]

Interestingly, EH-MSC administration also resulted in a significant upregulation of mTORC1, with the highest expression observed in the 300 µL group. While mTORC1 activation is commonly linked to cellular senescence and aging,transient or context-specific activation may promote anabolic repair processes, such as collagen synthesis and tissue regeneration.[10-12,26] Our findings are in agreement with a previous study,.which reported that EH-MSC injection significantly increased TGF-β levels and collagen density in Wistar rats with UVB-induced collagen loss, with the highest TGF-β concentration observed in the 300 µL EH-MSC group (155.56±99.84 pg/mL) and a significant increase in collagen density compared with the saline-treated group ($p$=0.000).24 This suggests that EH-MSCs can regulate both catabolic and anabolic processes in the extracellular matrix.

Moreover, hypoxia preconditioning appears to potentiate the therapeutic effects of exosomes, as EH-MSCs have been shown to exert stronger pro-angiogenic and regenerative effects than exosomes produced under normoxic conditions in preclinical models of tissue repair and wound healing.[27,28] Hypoxia-MSC exosomes have been

Print ISSN: 2527-4384, Online ISSN: 2527-3442
DOI: 10.21705/mcbs.v10n1.749

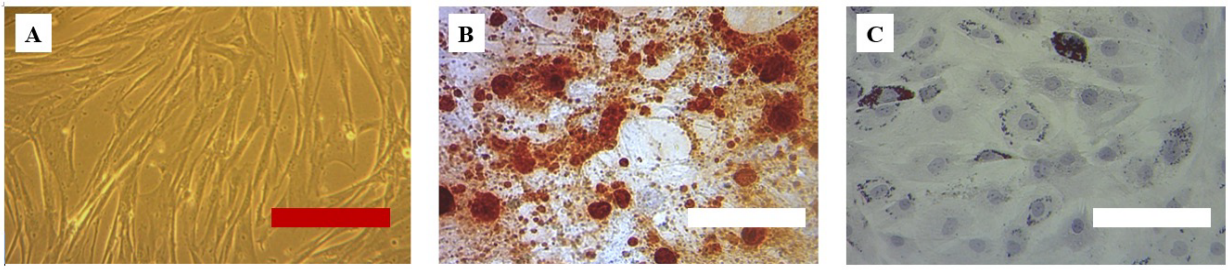


**Figure 3. Validation of hypoxia-conditioned MSCs.** A: MSCs at 80% confluence showing fibroblast-like morphology (40×). B: osteogenic differentiation indicated by calcium deposits stained with Alizarin Red (400×). C: adipogenic differentiation shown by lipid droplets stained with Oil Red O (400×). Red bar = 100 µm; white bar = 10

reported to reduce TNF-α while increasing VEGF in an alopecia model. These immunomodulatory actions parallel our observation of MMP-2 downregulation, suggesting that hypoxia conditioning enriches exosomal cargo with factors that both dampen inflammation and limit ECM degradation in UV-B–induced collagen loss.

Overall, these findings contribute novel insights by demonstrating that EH-MSCs can simultaneously downregulate MMP-2 and upregulate mTORC1 in UV-B–induced skin damage. This dual pathway modulation highlights a potential therapeutic mechanism whereby exosomes mitigate collagen degradation while promoting tissue repair. Importantly, the regenerative and immunomodulatory effects observed here are consistent with other studies, strengthening the translational relevance of EH-MSCs as a candidate therapy for photoaging.[23–25,29-30] Nevertheless, the paradoxical role of mTORC1 activation warrants careful interpretation. While chronic mTORC1 activation is deleterious, leading to reduced autophagy and accelerated aging, temporary stimulation may facilitate wound healing and extracellular matrix recovery.[31,32]

From a translational perspective, EH-MSCs may complement existing anti-photoaging approaches such as topical agents and injectable fillers that primarily target surface changes or hydration rather than upstream molecular pathways. In this model, the 300 µL EH-MSC dose produced greater mTORC1 upregulation and MMP-2 suppression than hyaluronic acid alone, indicating a more pronounced modulation of extracellular matrix remodeling (Table 2, Figure 5). As a cell-free product, exosome therapy may offer practical advantages over whole-cell MSC administration, including a potentially more favorable safety profile, the possibility of standardized large-scale production, and development as off-the-shelf formulations for clinical use.[15-16,23-24] However, the present experiment was not designed to systematically evaluate toxicity, immunogenicity, or long-term outcomes, and we did not perform formal dose-escalation or repeated-dosing studies;

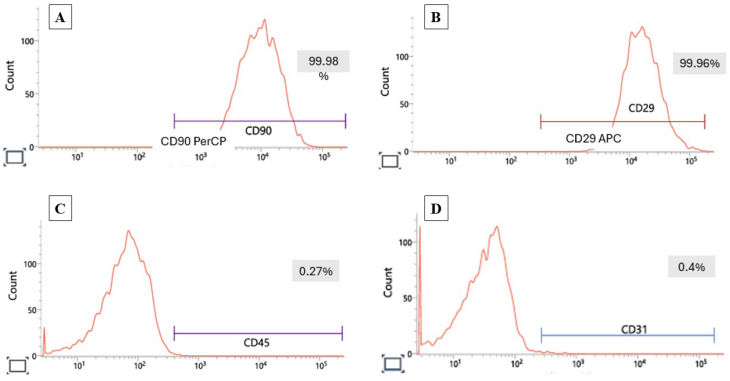


**Figure 4. Flow cytometry characterization of MSC surface markers.** (A) High expression of CD90 (99.98%) and (B) CD29 (99.96%) confirming positive mesenchymal markers. (C) Minimal expression of hematopoietic marker CD45 (0.27%) and (D) endothelial marker CD31 (0.4%) confirming negative markers. Results validate the MSC immunophenotype consistent with ISCT criteria.

**Table 2. Mean expression and statistical tests of mTORC1 and MMP-2 across groups.**

| Expression/Statistical Test | 200 µL Normal Saline (G2) | 200 µL Hyaluronic Acid (G3) | 200 µL EH-MSCs (G4) | 300 µL EH-MSCs (G5) | |
|---|---|---|---|---|---|
| **mTORC1** | 0.313 ± 0.057 | 0.498 ± 0.180 | 0.687 ± 0.223 | 1.088 ± 0.286 | |
| Shapiro wilk (*p*) | 0.102 † | 0.355 † | 0.162 † | 0.152 † | |
| Lavene test (*p*) | | | | | 0.077 ‡ |
| Oneway ANOVA (*p*) | | | | | <0.001* |
| Post hoc LSD (*p*) | | | | | |
| 200 µL Normal saline (G2) | | 0.133 | 0.005* | <0.001* | |
| 200 µL Hyaluronic acid (G3) | 0.133 | | 0.127 | <0.001* | |
| 200 µL EH-MSCs (G4) | 0.005* | 0.127 | | 0.003* | |
| **MMP-2** | 1.012 ± 0.177 | 0.595 ± 0.188 | 0.422 ± 0.099 | 0.187 ± 0.070 | |
| Shapiro wilk (*p*) | 0.223 † | 0.628 † | 0.366 † | 0.223 † | |
| Lavene test (*p*) | | | | | 0.009 |
| Oneway ANOVA (*p*) | | | | | <0.001* |
| Post hoc Tamhane's T2 (*p*) | | | | | |
| 200 µL Normal saline (G2) | | 0.017* | <0.001* | <0.001* | |
| 200 µL Hyaluronic acid (G3) | 0.017* | | 0,281944444 | 0.013* | |
| 200 µL EH-MSCs (G4) | <0.001* | 0,281944444 | | 0.006* | |

Note: † Normal ($p$>0.05); ‡ Homogen ($p$>0.05); * Significant difference ($p$<0.05)

these aspects, together with pharmacokinetics and delivery strategies, require dedicated investigation before clinical translation. In future, EH-MSC–based exosome formulations could be explored as adjunctive therapies for patients with UV-related skin damage or high photoaging risk, either in combination with standard photoprotective measures and dermatologic procedures or as minimally invasive regenerative interventions in early-stage photoaging.

This study had several limitations. First, the analysis was limited to gene expression, without confirming protein

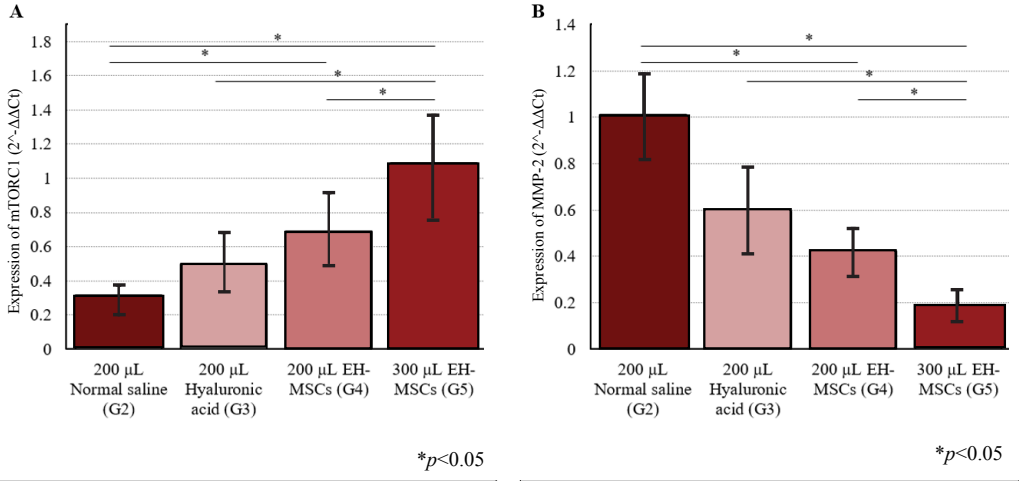


**Figure 3. Expression of mTORC1 and MMP-2 in different treatment groups.** A: mTORC1 expression was significantly increased in the 300 µL EH-MSCs group. B: MMP-2 expression showed a significant decrease in EH-MSC–treated groups (G4 and G5) compared to G2 and G3. Bars represent mean±SD; * indicates significant difference between groups (*$p$<0.05).

Print ISSN: 2527-4384, Online ISSN: 2527-3442
DOI: 10.21705/mcbs.v10n1.749

levels or functional outcomes such as collagen synthesis, enzymatic activity, or autophagy regulation. Second, we evaluated only two EH-MSC doses (200 μL and 300 μL), which were chosen to standardize injection volume across groups and to remain within a technically feasible, well-tolerated range for dorsal skin injections, but this limited dosing scheme may not fully capture the optimal therapeutic window. Third, exosome characterization was restricted to differential ultracentrifugation of MSC-conditioned medium without complementary analyses of tetraspanin or ESCRT-associated markers (e.g., CD9, CD63, CD81, TSG101, ALIX). Fourth, the study duration was relatively short, preventing evaluation of long-term efficacy or potential adverse effects of repeated administration. Finally, the use of an animal model, while necessary for mechanistic insight, may not fully replicate human photoaging, and further preclinical and clinical studies are required before translation to clinical application. Future studies should explore protein-level changes, long-term outcomes, and dose–response effects, as well as conduct translational research in human models to establish safety and efficacy for clinical application in UV-related skin aging.

## Conclusion

*C. racemosa* SPs exhibit dose-dependent anticancer activity against WiDr cells, with 500 μg/mL demonstrating significant viability reduction. The observed effects may be mediated through Caspase-3-dependent apoptosis, positioning these SPs as promising candidates for further colorectal cancer cells research.

## Authors' Contributions

Exosomes derived from EH-MSCs significantly downregulated MMP-2 expression while upregulating mTORC1 expression in a UV-B–induced collagen loss rat model, indicating dual protective effects through suppression of extracellular matrix degradation and potential stimulation of regenerative signaling. These findings highlight the novelty of EH-MSCs in simultaneously modulating catabolic and anabolic pathways, supporting their potential as a therapeutic s trategy for photoaging. Nevertheless, the complex role of mTORC1 activation warrants further investigation to clarify whether it contributes to tissue repair or pro-aging processes.

## Acknowledgment

This research did not receive any specific funding or support. The author assumes full responsibility for the content of this work.

## Authors' Contributions

ASF, AP, TS, and ES were involved in concepting and planning the research; ASF performed the data acquisition/ collection, calculated the experimental data, performed the analysis, drafted the manuscript and designed the figures, and interpreting the results. All authors took parts in giving critical revision of the manuscript.

## Ethical Statement

The study was approved by the Ethics Committee of the Faculty of Medicine, Universitas Islam Sultan Agung, Semarang, Indonesia (Approval No: 215/V/2025/Komisi Bioetik).

## Conflict of Interest

The authors declare that they have no conflicts of interest or competing interests related to the content of this manuscript.

## References

1. Bosch R, Philips N, Suárez-Pérez J, Juarranz A, Devmurari A, Chalensouk-Khaosaat J, *et al*. Mechanisms of photoaging and cutaneous photocarcinogenesis, and photoprotective strategies with phytochemicals. Antioxidants. 2015; 4(2): 248–68.
2. Mekić S, Jacobs LC, Gunn DA, Mayes AE, Ikram MA, Pardo LM, et al. Prevalence and determinants for xerosis cutis in the middle-aged and elderly population: a cross-sectional study. J Am Acad Dermatol. 2019 Oct;81(4):963-69.
3. Kursiussamawati FL, Primawati I, Sriwahyuni S. Knowledge level of dry skin care in the elderly at the koto tangah regional health center. Biomed J Indones. 2024; 10(1): 1–7.
4. Wei M, He X, Liu N, Deng H. Role of reactive oxygen species in ultraviolet-induced photodamage of the skin. Cell Div. 2024; 19(1): 1. doi: 10.1186/s13008-024-00107-z.
5. De Jager TL, Cockrell AE, Du Plessis SS. Ultraviolet light induced generation of reactive oxygen species. Cell Div. 2017; 996: 15–23.
6. Feng C, Chen X, Yin X, Jiang Y, Zhao C. Matrix Metalloproteinases on Skin Photoaging. J Cosmet Dermatol. 2024; 23(12): 3847–62.
7. Pittayapruek P, Meephansan J, Prapapan O, Komine M, Ohtsuki M. Role of matrix metalloproteinases in photoaging and photocarcinogenesis. Int J Mol Sci. 2016 2;17(6):868. doi: 10.3390/ijms17060868.
8. Ham SA, Yoo T, Hwang JS, Kang ES, Paek KS, Park C, *et al.* Peroxisome proliferator-activated receptor δ modulates MMP-

2 secretion and elastin expression in human dermal fibroblasts exposed to ultraviolet B radiation. J Dermatol Sci. 2014; 76(1): 44–50.
9. Yao C, Lee DH, Oh JH, Kim MK, Kim KH, Park CH, *et al*. Poly(I:C) induces expressions of MMP-1, -2, and -3 through various signaling pathways including IRF3 in human skin fibroblasts. J Dermatol Sci. 2015; 80(1): 54–60.
10. Colombero C, Remy D, Antoin BS, Macé A, Monteiro P, ElKhatib N, *et al*. mTOR Repression in Response to Amino Acid Starvation Promotes ECM Degradation Through MT1-MMP Endocytosis Arrest. Adv Sci. 2021; 8(17): e210614. doi: 10.1002/advs.202101614.
11. Laplante M, Sabatini DM. Regulation of mTORC1 and its impact on gene expression at a glance. J Cell Sci. 2013; 126(8): 1713-19.
12. Szwed A, Kim E, Jacinto E. Regulation and metabolic functions of mTORC1 and mTORC2. Physiol Rev. 2021; 101(3): 1371–426.
13. Vlassov A V., Magdaleno S, Setterquist R, Conrad R. Exosomes: current knowledge of their composition, biological functions, and diagnostic and therapeutic potentials. Biochim Biophys Acta - Gen Subj. 2012; 1820(7): 940–8.
14. Théry C, Witwer KW, Aikawa E, Alcaraz MJ, Anderson JD, Andriantsitohaina R, *et al.* Minimal information for studies of extracellular vesicles 2018 (MISEV2018): a position statement of the International Society for Extracellular Vesicles and update of the MISEV2014 guidelines. J Extracell Vesicles. 2018; 7(1): 1535750. doi: 10.1080/20013078.2018.1535750.
15. Wang T, Jian Z, Baskys A, Yang J, Li J, Guo H, *et al*. MSC-derived exosomes protect against oxidative stress-induced skin injury via adaptive regulation of the NRF2 defense system. Biomaterials. 2020; 257: 120264. doi: 10.1016/j.biomaterials.2020.120264.
16. Roszkowski S. Therapeutic potential of mesenchymal stem cell-derived exosomes for regenerative medicine applications. Clin Exp Med. 2024; 24(1): 46. doi: 10.1007/s10238-023-01282-z.
17. Hu S, Li Z, Cores J, Huang K, Su T, Dinh PU, *et al*. Needle-free injection of exosomes derived from human dermal fibroblast spheroids ameliorates skin photoaging. ACS Nano. 2019; 13(10): 11273–82.
18. Liang JX, Liao X, Li SH, Jiang X, Li ZH, Wu YD, *et al*. Antiaging properties of exosomes from adipos-derived mesenchymal stem cells in photoaged rat skin. Biomed Res Int. 2020; 2020(1): 6406395. doi: 10.1155/2020/6406395.
19. Liu W, Li L, Rong Y, Qian D, Chen J, Zhou Z, *et al*. Hypoxic mesenchymal stem cell-derived exosomes promote bone fracture healing by the transfer of miR-126. Acta Biomater. 2020; 103: 196–212.
20. Han Y, Ren J, Bai Y, Pei X, Han Y. Exosomes from hypoxia-treated human adipose-derived mesenchymal stem cells enhance angiogenesis through VEGF/VEGF-R. Int J Biochem Cell Biol. 2019; 109: 59–68.
21. Zou W, Lai M, Zhang Y, Zheng L, Xing Z, Li T, *et al*. Exosome release is regulated by mTORC1. Adv Sci. 2019; 6(3): 1801313. doi: 10.1002/advs.201801313.
22. Liu D, Kang H, Gao M, Jin L, Zhang F, Chen D, *et al*. Exosome transmitted circ_MMP2 promotes hepatocellular carcinoma metastasis by upregulating MMP2. Mol Oncol. 2020; 14(6): 1365–80.
23. Hariani NP, Putra A, Subchan P, Setiawan E. Mesenchymal stem cell-derived exosomes enhance FGF-1 and SDF-1 expression in rats with second degree burns. Mol Cell Biomed Sci. 2025; 9(2): 115-23.
24. Kusumawardani AIP, Subchan P, Sumarawati T, Setiawan E. Exosomes from hypoxic mesenchymal stem cells enhance TGF-β expression and promote collagen regeneration in wistar rats with collagen loss. Mol Cell Biomed Sci. 2025; 9(3): 141-8.
25. Andavania SJ, Syamsunarno MR, Putra A, Setiawan E. Hypoxia-induced mesenchymal stem cell exosomes modulate protein kinase A and VEGFR expression in ultraviolet b-induced hyperpigmentation in mice. Mol Cell Biomed Sci. 2025; 9(2): 91-7.
26. Smith P, Carroll B. Senescence in the ageing skin: a new focus on mTORC1 and the lysosome. FEBS J. 2025; 292(5): 960–75.
27. Su Y, Lu J, Liang F, Cheng J. Hypoxia-induced extracellular vesicles derived from human umbilical cord mesenchymal stem cells regulate macrophage polarization and enhance angiogenesis to promote diabetic wound healing. Biomolecules. 2025; 15(11): 1504. doi: 10.3390/biom15111504.
28. Liu P, Qin L, Liu C, Mi J, Zhang Q, Wang S, *et al*. Exosomes derived from hypoxia-conditioned stem cells of human deciduous exfoliated teeth enhance angiogenesis via the transfer of let-7f-5p and miR-210-3p. Front Cell Dev Biol. 2022; 10: 879877. doi: 10.3389/fcell.2022.879877.
29. Sulistami SM, Mulyani SP, Putra A, Setiawan E. Exosome Therapy from hypoxia-treated mesenchymal stem cells reduces TNF-α and increases VEGF levels in fluconazole-induced alopecia model. Mol Cell Biomed Sci. 2025; 9(3): 124-32.
30. Isfandiari AB, Putra A, Setiawan E. Hypoxia-exosome mesenchymal stem cells therapy reduces interleukin-6 levels and CD86 expression. Mol Cell Biomed Sci. 2025; 9(3): 133-40.
31. Jewell JL, Fu V, Hong AW, Yu FX, Meng D, Melick CH, *et al*. GPCR signaling inhibits mTORC1 via PKA phosphorylation of Raptor. Elife. 2019; 8. doi: 10.7554/eLife.43038.
32. Boutouja F, Stiehm CM, Platta HW. mTOR: A cellular regulator interface in health and disease. Cells. 2019; 8(1): 18. doi: 10.3390/cells8010018.